Searching for the triplet Higgs sector via central exclusive production at the LHC

Published by IOP Publishing for SISSA

Received: *January 30, 2009*
Revised: *April 3, 2009*
Accepted: *April 14, 2009*
Published: *May 5, 2009*

Searching for the triplet Higgs sector via central exclusive production at the LHC

M. Chaichian,[a] **P. Hoyer,**[a] **K. Huitu,**[a] **V.A. Khoze**[b,c] **and A.D. Pilkington**[c]

[a] *Department of Physics, University of Helsinki and Helsinki Institute of Physics, P.O. Box 64, FIN-00014 University of Helsinki, Finland*

[b] *Institute for Particle Physics Phenomenology, University of Durham, South Road, Durham, DH1 3LE, U.K.*

[c] *School of Physics and Astronomy, University of Manchester, Oxford Road, Manchester M13 9PL, U.K.*

E-mail: masud.chaichian@helsinki.fi, paul.hoyer@helsinki.fi, katri.huitu@helsinki.fi, v.a.khoze@durham.ac.uk, andrew.pilkington@cern.ch

Abstract: We discuss the prospects of searching for the neutral Higgs bosons of the triplet model in central exclusive production at the LHC. A detailed Monte Carlo analysis is presented for six benchmark scenarios for the Higgs boson, H_1^0, these cover $m_{H_1^0} = 120$, 150 GeV and doublet-triplet mixing of $c_H = 0.2$, 0.5 or 0.8. We find that, for appropriate values of c_H, an excellent Higgs mass measurement is possible for the neutral Higgs in the triplet model, and discuss how to distinguish the triplet model Higgs boson from the Higgs boson of the Standard Model.

Keywords: Higgs Physics, Beyond Standard Model

ArXiv ePrint: 0901.3746

doi:10.1088/1126-6708/2009/05/011

JHEP05(2009)011

Contents

JHEP05(2009)011

1 Introduction

It is expected that the nature of electroweak symmetry breaking will be revealed by the LHC experiments in the near future. In the Standard Model (SM), the electroweak symmetry is spontaneously broken by a Higgs doublet, which contains a neutral scalar field that acquires a vacuum expectation value (VEV). However, several Higgs multiplets typically occur in extensions to the SM. In supersymmetric models, at least one additional doublet is required. In left-right symmetric models, triplets are added to naturally generate a small mass for the neutrinos. Although the new scalars do not always take part in the electroweak symmetry breaking, they affect the properties of the Higgs boson through mixing.

Models with an extended Higgs sector typically contain charged scalars. A large number of studies [1, 2] have previously investigated the possibility of studying the doubly or singly charged components of higher representation.[1] However the charged scalars may be considerably heavier than the light neutral bosons. Therefore, it would be instructive to

[1] For example the discovery of the $ZW^{(+-)}H^{(-+)}$ and/or $W^-W^-H^{++}$ vertices would serve as a direct proof of the non-standard structure of the Higgs sector (see e.g. [3]).

study the properties of the light neutral Higgs particles in order to reveal the manifestation of new representations [4].

Higgs triplets are an especially attractive possibility [5]. A tiny neutrino mass may indicate that the mass is being generated by the seesaw mechanism containing the coupling of neutrinos to the triplet. In addition, composite Higgs models contain several multiplets, including the triplet ones. Triplets also occur in the little Higgs models - see, for example, [6] and references therein.

Determining that a new detected state is indeed a Higgs boson and distinguishing it from the Higgs boson of the SM will be far from trivial. This task will require a comprehensive programme of precision Higgs measurements. In particular, it will be of utmost importance to determine the spin and CP properties of a new state and to measure precisely its mass, width and couplings. In this work, we suggest that the neutral sector of the triplet representation can be studied using the central exclusive production (CEP) mechanism (see, for example, [7]) if forward proton detectors are installed at ATLAS and/or CMS, (see [8]).

The structure of the paper is as follows. In section 2, we consider the general properties of models with higher representations. We then concentrate on the triplet representation in section 3; we choose a benchmark model with the electroweak ρ-parameter equal to unity at tree-level, although the results are quite general. In section 4, we introduce the central exclusive production process. Finally, in section 5, we present a detailed Monte Carlo analysis of the central exclusive production of a neutral Higgs boson in the triplet model for a selection of parameter choices.

2 Models with general Higgs representations

We start with the Standard Model gauge group $\mathrm{SU}(2)_L \times \mathrm{U}(1)_Y$ for the electroweak sector. The masses of the gauge bosons are then obtained from the kinetic part of Lagrangian,

$$L_{\mathrm{kin}} = \sum_k (D^\mu \phi_k)^* (D_\mu \phi_k) + \frac{1}{2} \sum_i (D^\mu \xi_i)^T (D_\mu \xi_i), \tag{2.1}$$

where ϕ_k are complex representations and ξ_i are real ones. The covariant derivative is

$$D_\mu = \partial_\mu + igW_\mu^a T^a + \frac{Y}{2} g' B_\mu, \tag{2.2}$$

where T^a is the generator of SU(2) in the appropriate representation (with $\mathrm{Tr}(T^a T^b) = \frac{1}{2}\delta^{ab}$) and Y is the U(1) hypercharge. Here W^a and B are the SU(2) and U(1) gauge bosons respectively, and the mixing angle θ_W of the Z boson and photon is obtained by diagonalizing the neutral sector. The W and Z boson masses are given by

$$m_Z^2 = (g^2 + g'^2) \sum_i T_{3i}^2 v_i^2, \quad m_W^2 = g^2 \sum_i T_{3i}^2 v_i^2, \tag{2.3}$$

where T_{3i} is the isospin third component and v_i is the VEV of particle i. It is clear from eq. (2.3) that the doublet VEV decreases when several representations obtain non-vanishing VEVs. Furthermore, since the left-handed fermions are in doublets, the charged fermions

JHEP05(2009)011

can only get their masses through the Higgs doublet representation,[2] $m_f = y_f v_{\text{doublet}}$, and the fermion Yukawa coupling, y_f, must increase to produce the fermion masses. This, for example, leads to an enhancement in the production cross section for Higgs production via gluon fusion, where the dominant contribution is due to the top quark loop. A further enhancement is present in the branching ratio to fermion anti-fermion pairs. The possibility arises, therefore, of observing a very different prediction to that of the Standard Model.

The higher Higgs representations are severely restricted by the electroweak ρ-parameter. The ρ-parameter in the Standard Model is defined by the ratio of the gauge boson masses,

$$\rho = \frac{m_W^2}{m_Z^2 \cos^2 \theta_W}, \tag{2.4}$$

which at tree level is exactly unity in the Standard Model. The radiative corrections to the ρ-parameter have been studied in the SM up to three-loop level [9] - [15].[3] For $m_H \sim 2m_W$, the correction to the ρ-parameter is $\rho - 1 \sim -0.00078$+(4-loop and higher corrections). For heavier Higgs masses, the absolute value of the negative corrections increase. In a model with several scalar representations, whose neutral component develops a VEV, the ρ-parameter is given at tree level by [18]

$$\rho = \frac{\sum_i r_i \left(T_i(T_i+1) - T_{3i}^2 \right) v_i^2 \right)}{\sum_i 2 T_{3i}^2 v_i^2}. \tag{2.5}$$

Here T_i is the weak isospin and $r_i = 1/2(1)$ for real (complex) representations (see eq. (3.1) for examples). Finally, the ρ-parameter is experimentally constrained to be [19],

$$\rho - 1 = 0.0002 \begin{array}{l} +0.0024 \\ -0.0009 \end{array}, \tag{2.6}$$

where the quoted errors are at 2σ. As the loop-corrections to the ρ-parameter in the SM are negative, it can be argued that the ρ-parameter favors either a light Higgs boson or models that result in positive corrections to ρ.

3 Higgs bosons in a triplet model

In order to fulfill the experimental constraint on the ρ-parameter in eq. (2.6), the triplet VEV has to be small. Using eqs. (2.5) and (2.6) one finds that the upper limit for the triplet VEV is a few GeV's assuming that there is one triplet in addition to one doublet. An alternative method to satisfy the experimental constraint at tree-level[4] is to have representations which add up to $\rho = 1$. We discuss this next.

[2] For the neutral fermions this is not the case, since the Majorana masses can be generated through triplets.

[3] An explicit formula for the one-loop correction $\Delta\rho^{(1)}$ in $\rho = \Delta\rho^{(1)} + \Delta\rho^{(2)} + \Delta\rho^{(3)}$ is given in [16], two-loop terms are given in [17], and three-loop corrections in [15].

[4] At one-loop level, one has to consider renormalization. It has been shown in [20] that $\rho \neq 1$ at tree-level is acceptable in a real triplet model as the experimental measurement of ρ is satisfied after calculating higher order corrections.

JHEP05(2009)011

3.1 A model with $\rho = 1$

We consider the model developed by Georgi and Machacek [1], and further studied in [21–23] in which additional representations are chosen in such a way that the tree-level value of ρ remains unity. The ρ-parameter is fixed to one by choosing one complex scalar doublet ($\phi_{Y=1}$) and two triplets, one real ($\xi_{Y=0}$) and one complex ($\chi_{Y=2}$). These can be written as

$$\phi = \begin{pmatrix} \phi^{0*} & \phi^{+} \\ \phi^{-} & \phi^{0} \end{pmatrix}, \quad \chi = \begin{pmatrix} \chi^{0} & \xi^{+} & \chi^{++} \\ \chi^{-} & \xi^{0} & \chi^{+} \\ \chi^{--} & \xi^{-} & \chi^{0*} \end{pmatrix}. \tag{3.1}$$

The following sign conventions are chosen: $\phi^- = -(\phi^+)^*$, $\chi^{--} = (\chi^{++})^*$, $\chi^- = -(\chi^+)^*$, $\xi^- = -(\xi^+)^*$, and $\xi^0 = (\xi^0)^*$. The VEVs of the neutral components of the Higgs fields are denoted by $\langle\chi^0\rangle = \langle\xi^0\rangle = b$ and $\langle\phi^0\rangle = a/\sqrt{2}$. For doublet-triplet mixing, the standard notation is employed:

$$c_H \equiv \frac{a}{\sqrt{a^2+8b^2}}, \quad s_H \equiv \frac{\sqrt{8}b}{\sqrt{a^2+8b^2}}, \quad v^2 \equiv a^2 + 8b^2. \tag{3.2}$$

The most general scalar potential for the model, assuming invariance under $\chi \to -\chi$, is

$$\begin{aligned} V \;=\; & \lambda_1(\mathrm{Tr}\phi^\dagger\phi - c_H^2 v^2)^2 + \lambda_2\left(\mathrm{Tr}\chi^\dagger\chi - \frac{3}{8}s_H^2 v^2\right)^2 \\ & + \lambda_3\left(\mathrm{Tr}\phi^\dagger\phi - c_H^2 v^2 + \mathrm{Tr}\chi^\dagger\chi - \frac{3}{8}s_H^2 v^2\right)^2 \\ & - \lambda_4\left(\mathrm{Tr}\phi^\dagger\phi\mathrm{Tr}\chi^\dagger\chi - 2\sum_{ij}\mathrm{Tr}(\phi^\dagger\tau_i\phi\tau_j)\mathrm{Tr}(\chi^\dagger t_i\chi t_j)\right) \\ & + \lambda_5\left(3\mathrm{Tr}(\chi^\dagger\chi\chi^\dagger\chi) - (\mathrm{Tr}\chi^\dagger\chi)^2\right), \end{aligned} \tag{3.3}$$

where $\tau_i/2$ are the SU(2) generators in the doublet representation and t_i in the triplet representation.

As we are interested in this model mainly to illustrate the possibility of studying a neutral triplet Higgs sector, it is enough to limit ourselves to the case in which λ_3 is zero and $\lambda_4 = \lambda_5$. The tree-level results of this triplet model are sufficient for demonstrating the phenomenology of the higher representations. In this case, the neutral doublet and triplet do not mix and the neutral mass eigenstates are

$$\begin{aligned} H_1^0 &= \phi^{0r}, & H_1^{0\prime} &= \frac{1}{\sqrt{3}}(\sqrt{2}\chi^{0r} + \xi^0), \\ H_3^0 &= c_H\chi^{0i} + s_H\phi^{0i}, & H_5^0 &= \frac{1}{\sqrt{3}}(\sqrt{2}\xi^0 - \chi^{0r}), \end{aligned} \tag{3.4}$$

where $\chi^0 = (\chi^{0r} + i\chi^{0i})/\sqrt{2}$. The masses of the neutral scalars are

$$\begin{aligned} m^2_{H_1^0} &= 8c_H^2\lambda_1 v^2, & m^2_{H_1^{0\prime}} &= 3s_H^2\lambda_2 v^2, \\ m^2_{H_3^0} &= \lambda_4 v^2, & m^2_{H_5^0} &= 3(\lambda_5 s_H^2 + \lambda_4 c_H^2)v^2. \end{aligned} \tag{3.5}$$

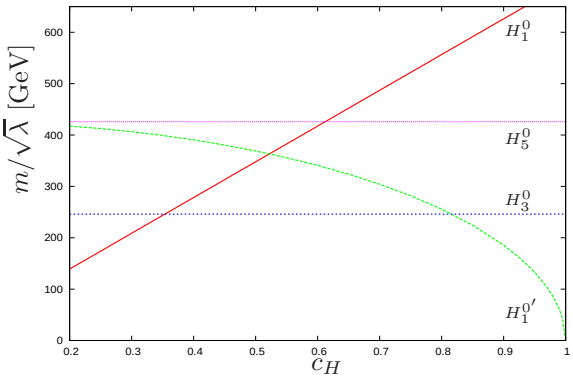

Figure 1. Masses of the Higgs bosons, m_{H_i}, divided by the unknown $\sqrt{\lambda_i}$ couplings, as a function of c_H.

The lightest neutral scalar can be H_1^0 if either c_H or λ_1 is small - the $m/\sqrt{\lambda_i}$ values are shown in figure 1. It should be noted that charged scalars exist with the same masses as H_3^0 and H_5^0.

The couplings of the neutral scalars to the fermions and the gauge bosons are

$$
\begin{aligned}
&H_1^0 q\bar{q} : -\frac{g m_q}{2 m_W c_H}, && H_3^0 t\bar{t} : \frac{i g m_t s_H}{2 m_W c_H}\gamma_5, && H_3^0 b\bar{b} : -\frac{i g m_b s_H}{2 m_W c_H}\gamma_5,\\
&H_1^0 W^+W^- : g m_W c_H, && H_1^0 ZZ : \frac{g}{\cos^2\theta_W} m_W c_H, &&\\
&H_1^{0\prime} W^+W^- : \frac{2\sqrt{2}}{\sqrt{3}} g m_W s_H, && H_1^{0\prime} ZZ : \frac{g 2\sqrt{2}}{\cos^2\theta_W \sqrt{3}} m_W s_H, &&\\
&H_5^0 W^+W^- : \frac{1}{\sqrt{3}} g m_W s_H, && H_5^0 ZZ : -\frac{2g}{\cos^2\theta_W \sqrt{3}} m_W s_H. &&
\end{aligned}
\tag{3.6}
$$

It is clear that, at tree-level, the coupling of the H_1^0 to fermions is always enhanced by the factor of $1/c_H$. Conversely, the coupling of the H_3^0 to fermions is either enhanced or suppressed, depending on the ratio of s_H and c_H, and the other neutral scalars do not couple to fermions. Importantly, the gauge boson couplings to H_1^0 are suppressed by a factor c_H with respect to the SM and the role of vector boson fusion mechanism for H_1^0 production is reduced if c_H is small. The other Higgs couplings to gauge bosons are suppressed by s_H. The $Hq\bar{q}$ couplings presented in figure 2 (a) are considerably enhanced for small c_H in comparison to the SM prediction. In figure 2 (b), the HVV couplings are shown, again normalized to the SM couplings.

3.2 Decays of H_1^0 and constraints on the parameters

In this section, we consider the H_1^0 Higgs boson, which becomes the Standard Model Higgs boson for vanishing doublet-triplet mixing. The mass limits for H_1^0 can be deduced from the LEP results. The couplings of the H_1^0 to the gauge bosons are smaller than in the SM, leading to reduced production of Higgs bosons in Higgsstrahlung process [24], through which the Higgs was expected to be produced at LEP. The Higgs boson branching ratio to $b\bar{b}$ is 74% for $m_H = 114\,\text{GeV}$ in the Standard Model. Together with other fermions,

JHEP05(2009)011

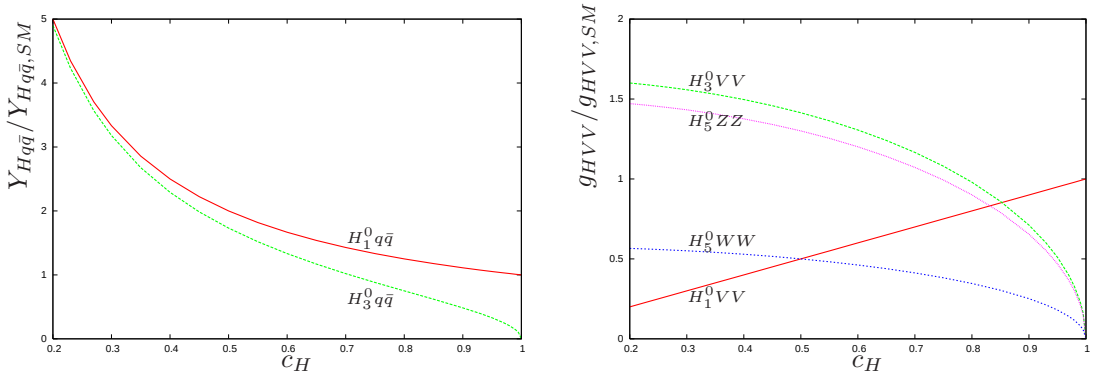

Figure 2. Couplings of the Higgs bosons to fermions (a) and gauge bosons (b), normalized by the Standard Model couplings.

the $b\bar{b}$ decay mode gives the main contribution to the total width of the Higgs boson, and, thus, the Higgs branching ratio does not change very much with c_H: for $m_H = 114\,\text{GeV}$ the branching ratio changes to 80% (81%) for $c_H = 0.5$ ($c_H = 0.2$). If the Higgs boson is lighter, the change is less. If we assume that the number of b-quark pairs gives the Higgs boson mass limit, it must be heavier than 73 GeV (40 GeV) for $c_H = 0.5$ ($c_H = 0.2$). Unitarity further constrains most masses, requiring them to be less than of the order of 1 TeV [23, 25].

The Yukawa couplings are constrained by perturbativity, which limits the H_1^0 coupling to top,

$$\frac{g m_{\text{top}}}{2 m_W c_H} < \sqrt{4\pi}. \tag{3.7}$$

From this it follows that $c_H > 0.2$, which currently is the most stringent limit for c_H.[5] The latest 95% confidence limit for the cross section × branching ratio of $pp \to H \to \tau\tau$ for a 120 GeV Higgs boson is observed by the D0 Collaboration to be approximately 5 pb given 2.2 fb^{-1} of data [27]. The CDF Collaboration observe a similar limit with 1.8 fb^{-1} of data. Although this offers no sensitivity to a SM Higgs boson, which has a production cross section of ∼1 pb and a branching ratio of ∼7%, one would expect increased sensitivity for the H_1^0 in the triplet model for small c_H (the production cross section is increased by a factor of $1/c_H^2$ w.r.t to the SM as the main production channel would be gluon-gluon fusion via a top quark loop). Thus it seems likely that the final combined CDF/D0 results will further constrain the lower c_H limit given the expected integrated luminosity of 8 fb^{-1} per experiment.

When calculating the branching ratios, it is necessary to consider also the loop induced decays of the Higgs bosons to gluons and photons. As mentioned, the tree-level gauge boson couplings to H_1^0 are suppressed by a factor c_H. The $\gamma\gamma H_1^0$ coupling is more complicated. In the SM, the W-loop gives the dominant contribution to the $\gamma\gamma H$ coupling. In the triplet model however, the fermion coupling is enhanced and the W-coupling suppressed for small

[5] Constraints from low energy precision measurements have been obtained from $Zb\bar{b}$ vertex, meson-antimeson mixing and ratios of $b \to u$ to $b \to c$ decays [26]. The radiative corrections to the $Zb\bar{b}$ vertex give the strongest constraint. Assuming $m_{H_3} \sim 1\,\text{TeV}$, one finds $\cos\theta_H > 0.3$ with 99.9 % C.L. However, since we consider only tree-level results in this work, we have not used this bound.

JHEP05(2009)011

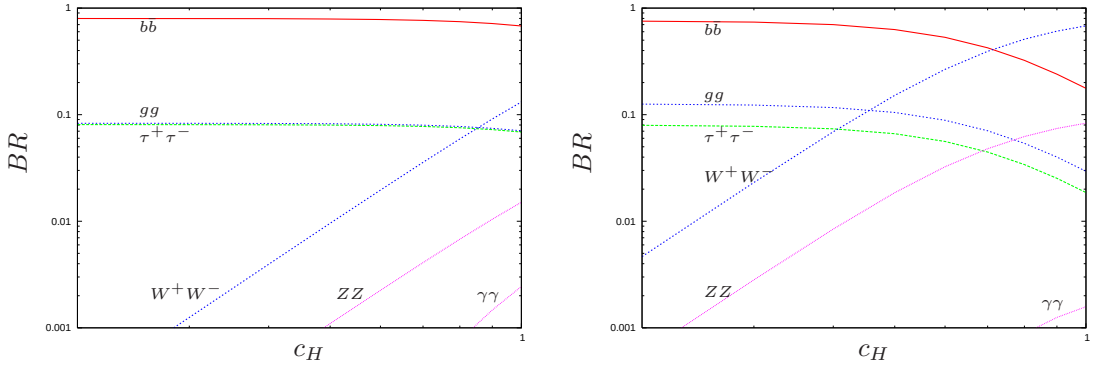

Figure 3. Branching ratios of H_1^0 to the Standard Model particles for $m_H = 120\,\text{GeV}$ (a) and $m_H = 150\,\text{GeV}$ (b).

values of c_H, so that the top loop becomes more important and the $\gamma\gamma H_1^0$ coupling is enhanced for small c_H. However, since the total width increases when c_H decreases, the branching ratio to photons remains smaller than in the SM. The gluon coupling to H_1^0 is enhanced by $1/c_H$ due to the fermion loop. These effects are seen in figure 3, where the branching ratios of H_1^0 are presented for $m_{H_1^0} = 120\,\text{GeV}$ and $150\,\text{GeV}$.

4 Central exclusive diffractive production of the triplet Higgs boson

The central exclusive production (CEP) of a Higgs boson is defined as $pp \to p \oplus H \oplus p$, where the $\oplus$ denote the presence of large rapidity gaps between the outgoing protons and the decay products of the central system. It has been suggested in recent years that CEP offers a unique complimentary measurement to the conventional Higgs search channels, see for example, [7, 8, 28] - [33]. Firstly, if the outgoing protons scatter through small angles then, to a very good approximation, the primary active di-gluon system obeys a $J_z = 0$, CP-even selection rule [34]. Here J_z is the projection of the total angular momentum along the proton beam axis. The observation of the Higgs boson in the CEP channel therefore determines the Higgs quantum numbers to be $J^{\text{PC}} = 0^{++}$. Secondly, because the process is exclusive, all of the energy/momentum lost by the protons during the interaction goes into the production of the central system. Measuring the outgoing proton allows the central mass to be measured to just a few GeV, regardless of the decay products of the central system. A mass measurement of this type will require new forward proton detectors to be installed at ATLAS and/or CMS, which we discuss further in section 5.1.

For a Standard Model Higgs boson, central exclusive diffraction could allow the main decay channels ($b\bar{b}$, WW and $\tau\tau$) to be observed in the same production channel, which provides the opportunity to study the Higgs coupling to b-quarks. This may be very difficult to access in other search channels at the LHC, despite the fact that $H \to b\bar{b}$ is by far the dominant decay mode for a light SM Higgs boson. Furthermore, CEP can provide valuable information on the Higgs sector of MSSM, NMSSM and other popular BSM scenarios [31–33, 35–37]. In this paper, we propose that CEP is also beneficial if higher representations

JHEP05(2009)011

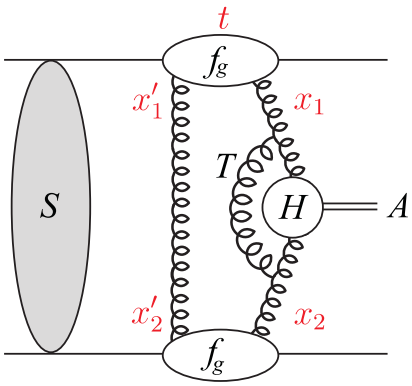

Figure 4. A symbolic diagram for the central exclusive production of a Higgs boson H.

of the Higgs sector are realized, in particular, in searches for the Higgs triplets discussed in section 3.

The theoretical formalism [38] - [42] for central exclusive production contains distinct parts, as illustrated in figure 4. The cross section can be written in the form [7, 38]

$$\sigma(pp \to p + H + p) \;\sim\; \frac{\langle S^2 \rangle}{B^2} \left| N \int \frac{dQ_t^2}{Q_t^4} f_g(x_1, x_1', Q_t^2, \mu^2) f_g(x_2, x_2', Q_t^2, \mu^2) \right|^2 \qquad (4.1)$$

where $B/2$ is the t-slope of the proton-Pomeron vertex, $\langle S^2 \rangle$ is the soft-survival probability and the normalization, N, is given in terms of the $H \to gg$ decay width. The amplitude-squared factor, $|\ldots|^2$, can be calculated in perturbative QCD because the dominant contribution to the integral comes from the region $\Lambda^2_{\rm QCD} \ll Q_t^2 \ll m_H^2$ for the large Higgs mass values of interest. The probability amplitudes, f_g, to find the appropriate pairs of t-channel gluons (x_1, x_1') and (x_2, x_2') are given by skewed unintegrated gluon densities at a hard scale $\mu \sim m_H/2$. It is important to emphasize, that these generalized gluon distributions are usually taken at $p_t = 0$, and then the "total" exclusive cross section is calculated by integrating over the transverse momentum, p_T, of the recoil protons. Assuming an exponential behaviour results in

$$\int dp_T^2 \; e^{-Bp_T^2} \;=\; 1/B \;=\; \langle p_T^2 \rangle. \qquad (4.2)$$

Thus, the additional factor in eq. (4.1) is not just the gap survival but rather the factor $\langle S^2 \rangle / B^2$ [7, 43], which has the form $S^2 \langle p_t^2 \rangle^2$ and is much less dependent on the parameters of the soft model [41, 43, 44]

The production cross section for Higgs bosons produced by gluon-gluon fusion and decaying to $b\bar{b}$ is proportional to

$$\frac{\Gamma^{\rm eff}}{m_H^3} \equiv \frac{\Gamma(H \to gg)}{m_H^3} BR(H \to b\bar{b}) \qquad (4.3)$$

where $\Gamma(H \to gg)$ is the decay width to gluons and $\mathrm{BR}(H \to b\bar{b})$ is the branching ratio to $b\bar{b}$ quarks. Table 1 shows the value of these parameters for the SM Higgs and the lightest

JHEP05(2009)011

	$m_H = 120\,\text{GeV}$		$m_H = 150\,\text{GeV}$	
	$\Gamma(H \to gg)$	$\text{BR}(H \to b\bar{b})$	$\Gamma(H \to gg)$	$\text{BR}(H \to b\bar{b})$
$c_H = 0.2$	6.35×10^{-3}	0.80	1.22×10^{-2}	0.75
$c_H = 0.5$	1.01×10^{-3}	0.79	1.95×10^{-3}	0.63
$c_H = 0.8$	3.97×10^{-4}	0.74	7.63×10^{-3}	0.32
SM	2.49×10^{-4}	0.68	4.79×10^{-4}	0.18

Table 1. The H_1^0 partial decay width to gluons (expressed in GeV) and branching ratio to $b\bar{b}$ for specific values of Higgs mass and c_H. The Standard Model (SM) prediction is shown for comparative purposes.

Higgs, H_1^0, in the triplet model. The central exclusive $H \to b\bar{b}$ cross section can therefore be enhanced by a large factor with respect to the Standard Model - we discuss this further in section 5

The CEP formalism has been extensively checked using the diffractive production of J/ψ and the leading neutron spectra [45] at HERA and the CDF data on central exclusive production processes [46] - [48]. Further tests of the formalism using the early LHC data have also been suggested [42]. The main uncertainties are associated with:

- The probability $\langle S^2 \rangle$ that additional secondaries will not populate the gaps.
- The probability to find the appropriate gluons that are given by generalized, unintegrated distributions $f_g(x, x', Q_t^2)$.
- Higher order QCD corrections to the hard subprocess, in particular, the Sudakov suppression.
- The so-called 'enhanced absorptive corrections' [41, 49, 50] and other effects that may violate the soft-hard factorization.

Let us focus first on the gap survival factor $\langle S^2 \rangle$. Since soft physics is involved, we need a reliable model of soft interactions to quantify the role of the absorption effects. In [39–41] soft interaction models were developed and tuned to describe all the available high energy soft pp interaction data. These models account for

(i) elastic rescattering (with the two protons in intermediate states),

(ii) the probability of low-mass proton excitations, and

(iii) the screening corrections due to high-mass proton dissociation (enhanced absorption).

The first two effects result in the so-called eikonal contribution, $\langle S^2_{\text{eik}} \rangle$. In the most recent version of the soft rescattering model [41, 44], the KMR group obtained $\langle S^2_{\text{eik}} \rangle_{\text{eff}} = 0.025$ when adjusting $\langle S^2_{\text{eik}} \rangle$ to its value corresponding to an exponential slope $B = 4\,\text{GeV}^{-2}$.

In the presence of enhanced screening, however, there is no longer exact factorisation between the hard and soft parts of the process, see for example [41, 45, 50]. The latest calculations [41] indicate that, in the case of the SM Higgs production at the LHC, the

JHEP05(2009)011

effective survival factor, due to both eikonal and enhanced rescattering, is $\langle S^2 \rangle_{\rm eff} \simeq 0.015 \pm 0.01$. It should be noted that the exclusive dijet, $\gamma\gamma$ and χ_c production data from CDF and the leading neutron data at HERA indicate that $\langle S^2_{\rm enh} \rangle$ is somewhat larger than this estimate, such that $\langle S^2 \rangle_{\rm eff}$ is nearer the upper limit of the quoted interval. In any case, it will be possible to measure $\langle S^2_{\rm enh} \rangle$ using early LHC data [42, 51].

As the generalized, unintegrated gluon distribution f_g has not been measured explicitly, it is obtained in the KMR approach [7, 38] from the conventional gluon distribution, $g(x, Q_t^2)$, known from the global parton analyses. The main uncertainty comes from the lack of knowledge of the integrated gluon distribution at low x and small scales. It was found in [42] that a variety of recent global analyses give a spread of

$$xg \;=\; (3 - 3.8) \;\; \text{for} \;\; x = 10^{-2} \quad \text{and} \quad xg \;=\; (3.4 - 4.5) \;\; \text{for} \;\; x = 10^{-3} \tag{4.4}$$

for $Q_t^2 = 4\,\text{GeV}^2$. These are big uncertainties bearing in mind that the CEP cross section depends on $(xg)^4$. A similar estimate of the uncertainty from the input gluon distribution functions was presented in [33]. The uncertainty related to the Sudakov factor is addressed in [42], along with the measurements that could reduce the uncertainty using early LHC data.

The overall uncertainty factor in the calculation of the CEP of Higgs bosons at the LHC was estimated to be approximately 2.5 in [31, 35]. Again, we note that the first LHC runs will allow the accuracy to be drastically improved.

5 Simulation of Higgs production in the triplet model

5.1 Forward proton tagging

The forward proton detectors will need to be installed in the high dispersion regions 220 m and 420 m either side of the interaction point at ATLAS and/or CMS.[6] We restrict our discussion and analysis to the ATLAS interaction point (IP), and note that a similar result would be obtained at CMS. There are three important aspects of forward proton tagging at the LHC that need to be considered for the purposes of this analysis; the acceptance and resolution of the proposed forward proton detectors and the ability of the detectors to measure the time-of-flight of each proton from the interaction point.

The acceptance of the forward proton system depends on the distance that each active detector is from the LHC beam. We choose the proton detectors located at 220 m (420 m) from the IP to be 2 mm (5 mm) from the beam and use the FPtrack program [52] to track the path of the protons through the LHC lattice in order to fully determine the acceptance. The acceptance of the forward proton detector system is dependent on the mass of the centrally produced object, M, which is given by

$$M^2 = \xi_1 \, \xi_2 \, s \tag{5.1}$$

where ξ_1 and ξ_2 are the fractional longitudinal momentum losses of the outgoing protons. For central masses less than 200 GeV, the protons are either both detected at 420m

[6] We refer the reader to the FP420 R&D report for more details on the detectors [8].

$\sigma_{H\to b\bar{b}}$ (fb)	$m_H = 120\,\text{GeV}$	$m_H = 150\,\text{GeV}$
$c_H = 0.2$	113.5	55.2
$c_H = 0.5$	18.0	7.4
$c_H = 0.8$	6.6	1.5

Table 2. Generator level cross sections, $\sigma_{H\to b\bar{b}}$, for central exclusive Higgs boson production for $m_H = 120, 150\,\text{GeV}$ and $c_H = 0.2, 0.5, 0.8$.

(symmetric tagging) or one is detected at 220 m and one at 420 m (asymmetric tagging). For example, the acceptance for a central mass of 120 GeV is approximately 28% for symmetric events and 20% for asymmetric events[7] [8]. This acceptance changes to 20% and 40% respectively for a 150 GeV central mass. Furthermore, symmetric and asymmetric events also have different mass resolution for a given central mass; the resolution of a 150 GeV Higgs boson is approximately 1.5 GeV and 4 GeV for symmetric and asymmetric proton tagging respectively.

Finally, the forward proton detectors will be capable of measuring the time-of-flight of each proton from the interaction point to an accuracy of 10 ps. The difference in the time-of-flight measurement of the protons gives a measurement of the interaction vertex to 2.1 mm, assuming that the reference timing system has negligible jitter. This vertex reconstruction proves to be very useful in background rejection, as discussed in section 5.3.

5.2 Signal and background event generation

The central exclusive signal and background events are simulated with full parton showering and hadronization effects using the ExHuME v1.3.4 event generator [53]. ExHuME contains a direct implementation of the KMR calculation [7, 38] of central exclusive diffraction given in section 4. The CTEQ6M [54] parton distribution functions are used to calculate the generalized gluon distributions, f_g. The generator level cross sections for central exclusive $H \to b\bar{b}$ production in the triplet model are presented in table 2 for $m_H = 120, 150$ GeV and $c_H = 0.2, 0.5, 0.8$. In section 5.5 we will present results for each of these parameter choices.

The backgrounds to $H \to b\bar{b}$ can be broken down into three broad categories; central exclusive, double pomeron exchange and overlap. We use the ExHuME event generator for the central exclusive backgrounds. ExHuME contains the leading order calculation for central exclusive $b\bar{b}$ production. Recent results however [55], show that the one-loop corrections to this process reduce the cross section by a factor of approximately two. We normalize the $b\bar{b}$ events generated by ExHuME accordingly. Central exclusive gg production has a much larger cross section than $b\bar{b}$ and can act as a background when the gluon jets are mis-identified by the b-tagging algorithms. At ATLAS, the mis-identification rate for each gluon jet is 1.3% for a b-tagging efficiency of 60% [56]. We do not generate exclusive $c\bar{c}$ events for two reasons. Firstly, due to the $J_z = 0$ spin-selection rule [34], exclusive $c\bar{c}$ production is suppressed with respect to $b\bar{b}$ by a factor of m_c^2/m_b^2. Furthermore, the mis-tag rate for c-jets to be identified as b-jets is ∼10%. Thus, the background contribution from

[7] Dead material in the detectors at 220 m can reduce the acceptance for symmetric tagging. We do not consider that effect here.

JHEP05(2009)011

exclusive $c\bar{c}$ events is considered to be negligible in comparison to the exclusive $b\bar{b}$ events. Higher order events, such as $b\bar{b}g$ have been studied in [57] with the conclusion that these types of events should be negligible after all experimental cuts. The demonstration of this using event generators cannot be completed until the relevant processes are implemented into the ExHuME Monte Carlo.

Double pomeron exchange (DPE) is the process $pp \to p + X + p$, where the central system, X, is produced by pomeron-pomeron fusion. The pomeron is assigned a partonic structure and so there are always 'pomeron remnants' accompanying the hard scatter. DPE has been extensively studied in relation to $H \to b\bar{b}$ and it has been concluded that this background is negligible after appropriate experimental cuts [33, 58]. We do not consider these types of events further.

In addition to these standard backgrounds, we also examine the effect of the overlap backgrounds. This source of background is important when there are a large number of pp interactions in each bunch crossing at the LHC. The largest overlap background is a three-fold coincidence between two soft events ($pp \to pX$), which produce forward protons within the acceptance of the forward detectors, and an inelastic event, which produces the hard scatter $pp \to X$ and, thus, can mimic our signal. To simulate these events we use HERWIG [59] plus JIMMY [60] to generate $pp \to b\bar{b}$, using the tune (A) to Tevatron data [61]. The forward protons are then added into the event using the prescription given in [33], which also allows us to calculate the probability of the coincidence as a function of the LHC luminosity.

The overlap background is initially reduced using the vertex matching provided by the proton time-of-flight (TOF) information. As the protons do not come from the same interaction as the jets, the vertex reconstructed using TOF will not, in general, coincide with the di-jet vertex. Given a fast-timing resolution of 10 ps, a rejection factor of 18 (15) can be obtained at low (high) luminosity by requiring that the di-jet vertex be within $\pm$4.2mm of the 'fake' vertex reconstructed from TOF. Approximately 95% of the CEP events will be retained by this requirement.

We do not consider the backgrounds from two-fold coincidences. It was demonstrated in [33] that the largest of these backgrounds - the coincidence between a soft central diffractive scattering and a standard QCD $2 \to 2$ scattering - was at least a factor of five smaller than the threefold coincidence. Furthermore, as discussed in the FP420 R&D report [8], this background is (i) probably overestimated and (ii) will be additionally rejected by the charged track cut outlined in the next section.

When generating the event samples, we require that the central mass be in the range $80 < M < 250\,\text{GeV}$, which improves the event generator efficiency and is the broad region of interest for this study. To approximate the detector effects, we smear the energy, momenta and angles of each central final state particle according to the ATLAS detector resolution [62]. The outgoing forward proton momenta are smeared by the amount specified in [63]. A mid-point cone algorithm is then applied to the samples and events retained if the leading jet has transverse energy greater than 45 GeV. Finally, b-tagging efficiencies are imposed after matching the two leading jets to the partonic level.

JHEP05(2009)011

5.3 Experimental cuts

To enhance the signal, we follow the experimental method used in a previous study of $H \to b\bar{b}$ in the SM and the MSSM [33], which imposes a number of exclusivity cuts.[8] Firstly, the rapidity of the central system can be estimated from the forward proton detectors by

$$y = \frac{1}{2}\ln\left(\frac{\xi_1}{\xi_2}\right). \tag{5.2}$$

The difference, Δy, between this rapidity measurement and the average pseudo-rapidity of the di-jets should be approximately zero for an exclusive event, Exclusive candidates satisfy

$$\Delta y = \left| y - \left(\frac{\eta_1 + \eta_2}{2}\right)\right| \leq 0.06, \tag{5.3}$$

where η_1 and η_2 are the pseudo-rapidities of the leading jets.

The di-jet mass fraction, R_j, determines the fraction of the central mass that is contained within the di-jet system. R_j is an improved version of the R_{jj} variable [64], which was used by CDF in the search for exclusive di-jet events [46]. For an exclusive di-jet event, one expects all of the mass to be contained in the di-jets, and hence $R_j = 1$. However, parton showering/hadronisation effects can result in energy outside of the jets. Furthermore, detector resolution will smear the di-jet mass measurement. An exclusive event is defined to be

$$0.85 \quad \leq \quad R_j = \frac{2E_T^1}{M}\cosh\left(\eta_1 - \mathrm{y}\right) \quad \leq \quad 1.1, \tag{5.4}$$

where E_T^1 is the transverse energy of the leading jet.

The third exclusivity cut requires the di-jets to be back to back in azimuth, which reflects the suppression of initial state radiation for an exclusive di-jet event. The back to back requirement is

$$|\pi - \Delta\phi| \leq 0.15, \tag{5.5}$$

where $\Delta\phi$ is the azimuthal angle between the jets. It is also possible to examine each event for underlying event activity, caused by multiple parton-parton interactions. The exclusive events do not have these additional scatters because the proton remains intact. It is possible to reject inclusive events, and, hence, the overlap background, by requiring few charged tracks, N_C, associated with the di-jet vertex but outside of the jets. This definition is, of course, dependent on the jet algorithm used to define the jets. An algorithm independent approach is to examine the charged track activity perpendicular to the leading jet, $N_C^{\perp}$. In this approach, charged tracks are assigned to the underlying event if they satisfy

$$\frac{\pi}{3} \leq |\phi_k - \phi_1| \leq \frac{2\pi}{3} \quad \text{or} \quad \frac{4\pi}{3} \leq |\phi_k - \phi_1| \leq \frac{5\pi}{3}, \tag{5.6}$$

where ϕ_k is a the azimuthal angle of a charged track and ϕ_1 is the azimuthal angle of the leading jet. In this analysis, we identify exclusive events by

$$N_C \leq 3 \quad \text{and} \quad \mathrm{N_C^{\perp}} \leq 1. \tag{5.7}$$

[8] A somewhat different experimental method was discussed in [31]. However, the final experimental efficiency broadly agrees with that used here [8].

Generator	Process	$\sigma_{420-420}$ (fb)	$\sigma_{420-220}$ (fb)
ExHuME	$H \to b\bar{b}$	0.53	0.28
	$b\bar{b}$	0.53	0.27
	gg	1.08	0.91
Overlap (L)	$b\bar{b}$	0.07	0.09
Overlap (H)	$b\bar{b}$	11.0	13.7
Total bgrd (L)		1.68	1.27
Total bgrd (H)		12.6	14.9

Table 3. The final cross sections for the $H \to b\bar{b}$ ($m_H = 120\,\text{GeV}$, $c_H = 0.5$) and relevant backgrounds after the all cuts discussed in the text. The overlap backgrounds are defined at both low (L) and high (H) luminosity. All the backgrounds form a continuum over the range 80<M<250 GeV.

For completeness, in table 3 we present the final cross sections for the signal (m_H =120 GeV, $c_H = 0.5$) and background events. It should be noted that the signal is concentrated at $M = 120\,\text{GeV}$, whereas the backgrounds form a continuum across the mass range 80<M<250 GeV. For details on the efficiencies of the individual cuts, and motivation for the cut choices, we refer the reader to [33]. The overlap backgrounds are luminosity dependent and are presented for constant luminosities of 10^{33} cm^{-2} s^{-1} (low) and 10^{34} cm^{-2} s^{-1} (high).

5.4 Trigger strategies

A major experimental challenge for central exclusive jet analyses is developing a trigger strategy to retain enough events. At ATLAS, jets with $E_T \sim 50\,\text{GeV}$ are heavily prescaled in the level one (L1) trigger, due to the high rate and the lack of additional rejective power in the high level trigger (HLT). The total L1 rate allowed at ATLAS is 75-100 kHz, which must be reduced to ∼100 Hz after the HLT. In this section, we discuss three possible trigger strategies. The first possibility is to exploit the muon rich nature of $b\bar{b}$ events. The lowest muon threshold (MU6) at ATLAS is designed to retain 80% of muons with transverse momentum greater than 6 GeV. The single muon trigger efficiency for $b\bar{b}$ events is 11% [33]. In order to keep the L1 rate down it will be necessary to require that the event contains jet with $E_T > 40\,\text{GeV}$ in conjunction with the muon.

The second trigger strategy is to require a 40 GeV jet in conjunction with a proton tagged in a detector at 220 m from the interaction point.[9] This trigger has been extensively studied in previous work [65], and it is expected that the unprescaled L1 rate will be less than 1 kHz up to a luminosity of L=2×10^{33} cm^{-2} s^{-1}. This rate however, will scale with L^2 and the trigger may have to be prescaled to give a fixed rate at the highest luminosity. We will investigate two fixed rate triggers; R5 is a L1 rate of 5 kHz and R10 is a L1 rate of 10 kHz. The drawback of this trigger strategy is that the symmetric events will not be retained, which could potentially have a large impact for a light Higgs boson measurement.

[9]The information from the detectors at 420m will not reach the central trigger processor within the latency of 2.5μs and so cannot be used in the L1 decision.

JHEP05(2009)011

It will be possible to dramatically reduce any high L1 rate using additional information in the HLT. Firstly, requiring that there be a proton detected at 420 m and using time-of-flight information to match the vertices will reject the events by a factor of approximately 600 (60) at low (high) luminosity. A loose b-tagging requirement could also be added. Finally, the R_j and Δy cuts reject the overlap events by a factor of approximately 100 and could be used to further reduce the rate.

The final trigger strategy is to allow a larger L1 rate for the 40 GeV jets, which is then reduced in the HLT by requiring two in-time protons. This trigger has also been studied in previous work [33]. The advantage of this approach is that it would retain both symmetric and asymmetric events. The L1 rate for 40 GeV jets is expected to be approximately 25 kHz at low luminosity, rising to 250kHz at high luminosity. We define a trigger for 40 GeV jets, JR25, which has a fixed rate of 25 kHz.[10] This trigger would be unprescaled at low luminosity and prescaled by a factor of ten at high luminosity.

5.5 Significance of observation and expected mass distributions

In this section, we estimate the significance of observing a neutral Higgs boson in the triplet model for the parameter choices presented in section 5.2 and for the trigger strategies outlined in section 5.4. As the overlap background is luminosity dependent (table 3), we must specify how the data was collected. For example, we examine the significance for an integrated luminosity of 60 fb^{-1}, which corresponds to between three and four years of data acquisition given a peak luminosity of 2×10^{33} cm^{-2} s^{-1}. We also present results for 300 fb^{-1} of data, which corresponds to between three and four years of data acquisition given a peak luminosity of 10^{34} cm^{-2} s^{-1}. It should be noted, however, that the data acquisition at the LHC will not be collected at one specific luminosity. Firstly, the peak luminosity will increase during the lifetime of the LHC with an improved understanding of the machine. Secondly, during each store, the luminosity will decrease exponentially with a lifetime of approximately 14 hours. We crudely approximate these effects by defining that half the data is collected at the peak luminosity and half the data at 75% of the maximum.

The signal and background events that pass the selection criteria are normalized to an expected number, N, for each trigger/luminosity scenario, i.e.

$$N = L\sigma\epsilon,$$

where L is the total integrated luminosity, σ is the final cross section for each process as shown in table 3 and ϵ is the trigger efficiency. In the case of the overlap background, σ is dependent on the assumed peak luminosity as described above. The MC distributions are then used to predict the expected number of events in each bin of a mass distribution. A pseudo-experiment is then carried out by randomly picking a number of events for each bin in the mass distribution according to a Poisson distribution. The significance of each pseudo-experiment is then obtained by fitting the pseudo-data with a signal-plus-background function and a background-only function. The significance is estimated from

[10] It was shown in CMS-based study [66] that this rate can be reduced by a factor of two by requiring that the majority of the transverse energy in the detector be contained within the dijets - i.e. that $(E_T^1 + E_T^2)/H_T > 0.9$, where H_T is the scalar sum of transverse energy deposited in the detector [65].

JHEP05(2009)011

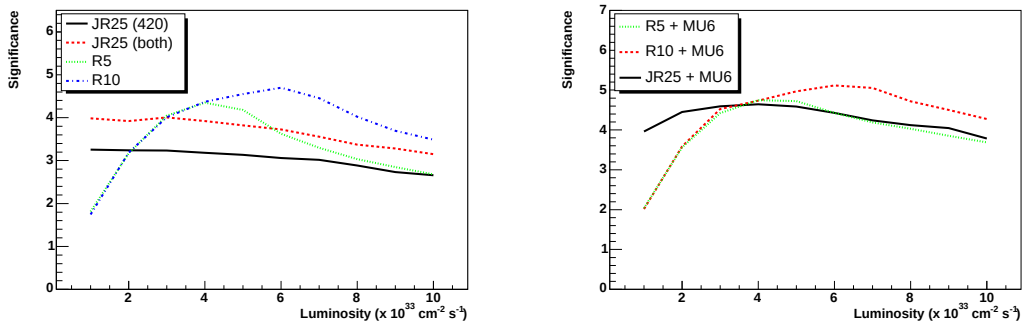

(a) **(b)**

Figure 5. (a) Expected significance ($m_H = 120\,\text{GeV}$, $c_H = 0.5$) for the R5, R10 and JR25 triggers as a function of luminosity given three years of data acquisition at each luminosity. We assume that $10\,\text{fb}^{-1}$ of data is collected each year per 10^{33} cm^{-2} s^{-1} of luminosity, i.e. $120\,\text{fb}^{-1}$ of data is collected at $4{\times}10^{33}$ cm^{-2} s^{-1}. (b) The significance of the R5, R10 and JR25 triggers when combined with the MU6 trigger.

the difference in χ^2 of the two fits by

$$S = \sqrt{\chi^2_b - \chi^2_{s+b}}. \tag{5.8}$$

We assume the background function will be well known from data - in this analysis we use the weighted MC background events to determine the shape and allow the normalization to vary.[11] The signal function is a Gaussian and all parameters are allowed to vary. We repeat the procedure for 500 pseudo-experiments to determine the average significance of each luminosity/trigger scenario and ensure that our results are consistent and the presented distributions typical.

To determine the significance for each parameter choice, the trigger strategies outlined in section 5.4 are evaluated and the best method chosen to retain the events. We choose the $m_H = 120\,\text{GeV}$, $c_H = 0.5$ point as our reference. Figure 5 (a) shows the significance as a function of luminosity for the R5, R10 and JR25 trigger strategies given three years of data acquisition at that luminosity. It is clear that the JR25 trigger is the best choice at low luminosity as it retains a high fraction of both symmetric and asymmetric events. At higher luminosities, the R5/R10 triggers become more favourable; the R5 (R10) trigger do not become prescaled until $4.5{\times}10^{33}$ cm^{-2} s^{-1} ($6.3{\times}10^{33}$ cm^{-2} s^{-1}) and the number of exclusive events in the final sample is increased even though the symmetric events are not retained. Figure 5 (b) shows the significance for R5, R10 and JR25 when combined with the MU6 trigger.

Figure 6 shows the expected mass distributions for $m_H = 120, 150\,\text{GeV}$ and $c_H = 0.2, 0.5$ for $60\,\text{fb}^{-1}$ of data collected at $2{\times}10^{33}$ cm^{-2} s^{-1} using a JR25+MU6 trigger. Example distributions for $c_H = 0.8$ are not shown as the calculated significance is less than 3σ. Figure 7 shows the same distributions but for $300\,\text{fb}^{-1}$ of data collected at 10^{34} cm^{-2} s^{-1} using the R10+MU6 trigger. A summary of the significance for each parameter choice

[11] We have checked our results using a quadratic background function and observe little difference.

JHEP05(2009)011

is presented in table 4 for both luminosity/trigger scenarios. The significance is approximately 4σ for the $c_H = 0.5$ parameter points and 12σ for the $c_H = 0.2$ parameter points.

For each parameter point, the information obtained from the fitting procedure in each pseudo-experiment can be used to obtain an RMS spread of Higgs masses. This gives a reasonable estimate of the error on the Higgs mass as measured by the forward proton detectors. Table 5 shows the RMS spread for each (significant) parameter choice. The R10 trigger strategy (used at high luminosity) retains only events with asymmetrically tagged protons, whereas the JR25 trigger (used at low luminosity) retains both symmetric and asymmetric events. Thus the high luminosity scenario in table 5 results in a poorer mass measurement than the low luminosity scenario because of the lower fraction of symmetric events in the sample. The final trigger strategy at ATLAS/CMS will have to balance the need for observation with the opportunity for more precise measurements. For all parameter choices the mass measurement can be made to better than 2 GeV; for $c_H = 0.2$ the mass measurement is better than 0.3 GeV.

It should be noted that the significances obtained for the $c_H = 0.2$ parameter points are well in excess of 10σ and the high rate triggers assumed in this analysis are not strictly needed for the measurement. Indeed, the MU6 trigger alone is capable of retaining enough events for the analysis - the significance for a 120 GeV Higgs boson is 4.5 for 60 fb^{-1} collected at 2×10^{33} cm^{-2} s^{-1}. The disadvantage is that the mass measurement is somewhat degraded, due to the reduced number of events.

The $c_H = 0.8$ points are observable if the overlap background can be additionally rejected. There are two possibilities related to improvements in the fast-timing system. Firstly, if the time-of-flight resolution of the forward detectors is improved, then both the vertex resolution and overlap rejection is improved by the same factor. Secondly, if the central jets can be timed to an accuracy of 70 ps, using optimal signal filtering in the ATLAS Liquid Argon Calorimeter [67], a factor of two rejection on the overlap background would be gained. If the central timing could be performed at the 10 ps level, then a factor of 12 rejection would be observed. The significance of the $c_H = 0.8$ parameter point for a 120 GeV Higgs boson increases to 3.2σ at high luminosity if the overlap background is additionally rejected by a factor of five. Improved overlap rejection would also increase the significance of the other parameter points at high luminosity.

6 Doubly charged Higgs bosons

An important feature of the triplet model is the existence of doubly charged Higgs bosons. Although not the focus of this paper, we comment on the possibility to observe these using the forward proton system discussed in section 5.1. The process of interest is $pp \to p \oplus H^{++}H^{--} \oplus p$, where the central system is produced via photon-photon fusion, i.e. $\gamma\gamma \to H^{++}H^{--}$. As two Higgs bosons are produced, the central system will be of higher mass than discussed in previous sections and at least one of the protons will be tagged by detectors placed at 220m from the IP.

The production cross section could be large [68]. It was shown in [8, 69] that the production cross section was 0.07 fb for a 200 GeV for singly charged scalar pair production.

JHEP05(2009)011

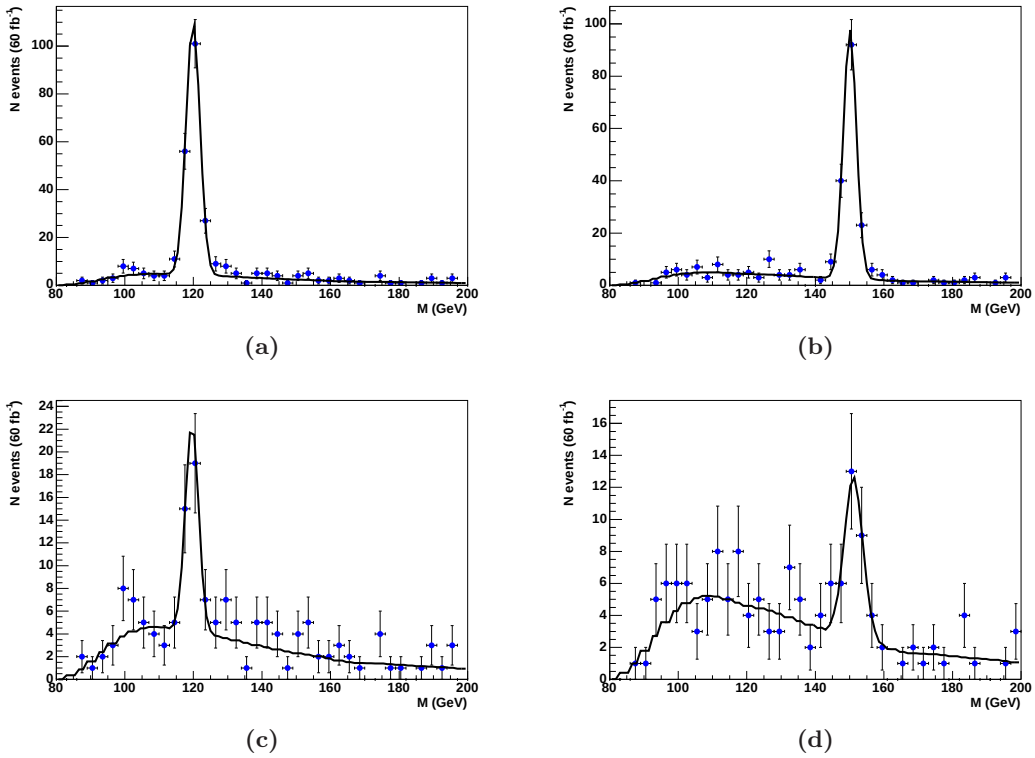

Figure 6. Expected mass distributions given $60\,\text{fb}^{-1}$ of data, collected at $2{\times}10^{33}$ cm^{-2} s^{-1} using a JR25+MU6 trigger, for the following parameter choices: (a) $m_H = 120\,\text{GeV}$ and $c_H = 0.2$, significance is 12.7σ (b) $m_H = 150\,\text{GeV}$ and $c_H = 0.2$, significance is 11.9σ. (c) $m_H = 120\,\text{GeV}$ and $c_H = 0.5$, significance is 4.5σ. (d) $m_H = 150\,\text{GeV}$ and $c_H = 0.5$, significance is 3.9σ.

m_H (GeV)	c_H	Significance (σ)	
		$60\,\text{fb}^{-1}$	$300\,\text{fb}^{-1}$
120	0.2	12.7	13.7
	0.5	4.5	4.3
	0.8	2.6	2.5
150	0.2	11.9	12.7
	0.5	3.9	4.3
	0.8	2.0	2.1

Table 4. Significance of central exclusive Higgs boson measurement for $m_H = 120, 150\,\text{GeV}$ and $c_H = 0.2, 0.5, 0.8$. The significance is obtained after using the cuts, trigger strategies and fitting procedure outlined in the text. As the overlap background is luminosity dependent, we present results for both $60\,\text{fb}^{-1}$ of data taken at a peak luminosity of $2{\times}10^{33}$ cm^{-2} s^{-1} and for $300\,\text{fb}^{-1}$ of data taken at a peak luminosity of 10^{34} cm^{-2} s^{-1}.

However, the cross section for doubly charged Higgs boson[12] pair production is a factor

[12]The doubly charged Higgs boson mass in the Machacek-Georgi model is the same as the H_5^0 scalar mass, and therefore, H^{++} with mass $m_{H^{++}} \sim 200 - 300\,\text{GeV}$ is possible, as it is heavier than the lightest

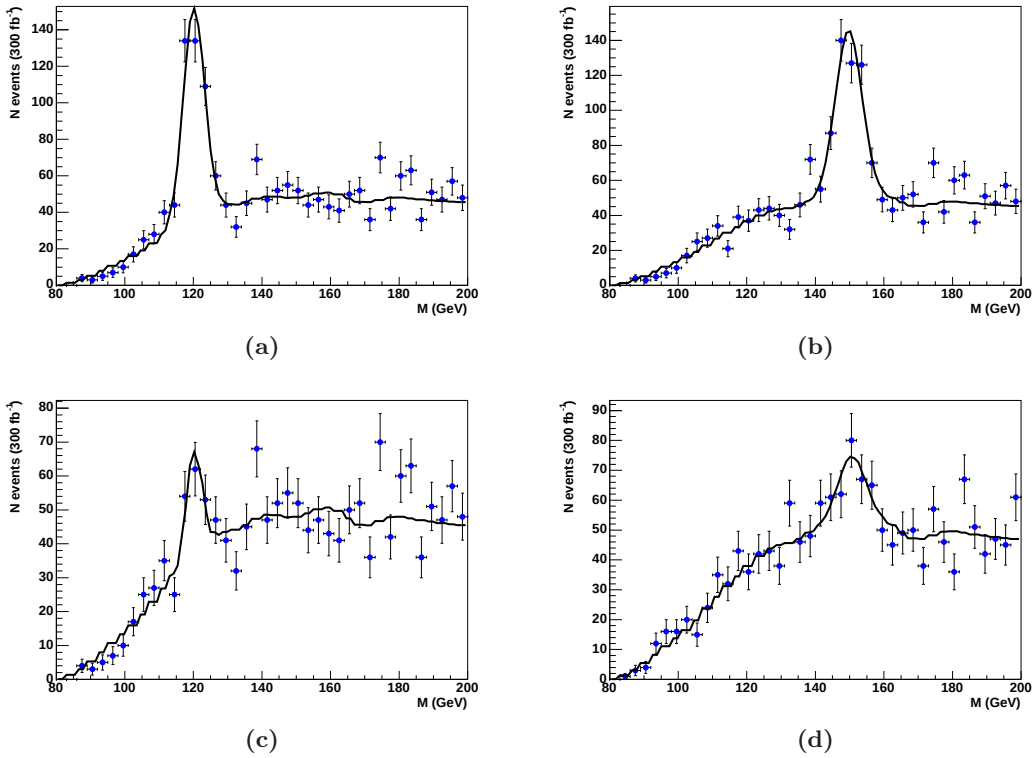

Figure 7. Expected mass distributions given 300 fb^{-1} of data, collected at 10^{34} cm^{-2} s^{-1} using a R10+MU6 trigger for the following parameter choices (a) $m_H = 120$ GeV and $c_H = 0.2$, significance is 13.7σ (b) $m_H = 150$ GeV and $c_H = 0.2$, significance is 12.7σ. (c) $m_H = 120$ GeV and $c_H = 0.5$, significance is 4.3σ. (d) $m_H = 150$ GeV and $c_H = 0.5$, significance is 4.3σ.

m_H (GeV)	c_H	σ_{m_H} (GeV)	
		60 fb^{-1}	300 fb^{-1}
120	0.2	0.2	0.3
	0.5	0.8	4.5
150	0.2	0.2	0.3
	0.5	1.8	2.4

Table 5. The error in the Higgs boson mass measurement, σ_{m_H}, estimated from the RMS spread of mass measurements made in the pseudo-experiments, for $m_H = 120, 150$ GeV and $c_H = 0.2, 0.5$. The 60 fb^{-1} of data (taken at a peak luminosity of 2×10^{33} cm^{-2} s^{-1}) uses a JR25 + MU6 trigger strategy whereas the 300 fb^{-1} of data (taken at a peak luminosity of 10^{34} cm^{-2} s^{-1}) uses R10 + MU6.

of 16 larger due to the factor of two increase in charge. Thus the cross section for pair-production of a 200 GeV doubly charged Higgs boson increases to 1.1 fb. It should be noted that the photon fusion production cross section decreases roughly by $\sim 1/M^3$ [7], and so the pair production of a 300 GeV doubly charged scalar would be approximately 0.3 fb.

neutral Higgs H_1^0.

JHEP05(2009)011

The forward proton acceptance for central systems in the range 400 GeV-1 TeV is better than 40% [63]. This means that we would expect more than 130 events with both outgoing protons measured for the pair production of a 200 GeV doubly charged Higgs boson given 300 fb^{-1} of data acquisition. This decreases to 40 events if the mass of the doubly charged Higgs is 300 GeV.

The events should be retained using the standard electron/muon trigger strategies currently in place at ATLAS/CMS. A doubly charged Higgs that is heavier than 200 GeV has several possible decay modes: $H^{++} \to W^+W^+$, W^+H^+, H^+H^+, l^+l^+. In any case, a high fraction of events will contain at least one electron/muon in the final state.

Therefore, forward proton tagging allows the possibility to study doubly charged scalars that are lighter than around 300 GeV. Note that, in exclusive production, the background conditions are more favourable in comparison to the conventional $pp \to H^{++}H^{--}X$ case considered e.g. in [68]. Also, in principle, the forward proton mode may allow to measure the $H^{\pm\pm}$ mass more accurately than in the inclusive case.

7 Conclusions

Searches for the manifestation of the extended Higgs sector at the LHC may allow new insight in the nature of electroweak symmetry breaking. The central exclusive production mechanism would provide a very powerful tool to complement the standard strategies at the LHC for studying Higgs particles. Here we focus on the production of the neutral Higgs boson of the triplet model in the forward proton mode. We assume a model with the tree-level value of the electroweak ρ-parameter consistent with experiment, $\rho = 1$. Although this model is used as a benchmark model for the triplets, our results are more general. An extra contribution from other representations enhances the doublet Yukawa couplings resulting in a different experimental signature to that of the SM. We show that a factor of two enhancement of the fermion couplings due to the higher representations implies a significant difference to the doublet case. Let us emphasize that in the case of the current model, all the fermion couplings to the Higgs boson, which is responsible for the fermion masses, increase. This is in contrast with, for instance, the MSSM, where couplings of up-type and down-type fermions change from the Standard Model differently, due to the fact that there are only doublets in the model. It is a common feature of higher Higgs representations that the doublet couplings are enhanced, which thus indicates that higher representations are involved.

We present a detailed Monte Carlo analysis of the central exclusive production of a triplet model Higgs boson for a number of parameter choices. For $c_H \leq 0.5$, we have shown that a light H_1^0 Higgs boson (of mass 120-150 GeV) can be observed with a 4σ (or better) significance if a fixed rate trigger is used. We find that a fixed rate *single jet* trigger is optimal at low luminosities whereas a fixed rate *forward proton* trigger (i.e. one proton detected at 220m in conjunction with a central jet) is optimal at high luminosities.

The expected error in the Higgs mass measurement using forward proton detectors is small. For $c_H = 0.2$, we find that the mass of the Higgs boson is measured to better than 0.3 GeV, regardless of the luminosity/trigger scenarios. This is due to the excellent mass

JHEP05(2009)011

resolution of the forward detectors and the large number of events. For $c_H = 0.5$, there are less events and so the error in the mass measurement increases. However, regardless of the parameter choice, the mass measurement can always be made to better than 2 GeV if a fixed rate single jet trigger is used to retain events in which both protons are tagged at 420 m from the IP.

Acknowledgments

We are grateful to Brian Cox, Albert De Roeck, Jeff Forshaw, John Gunion, Alan Martin, Risto Orava, Mark Owen, Misha Ryskin, Stefan Soldner-Rembold, and Marek Tasevsky for useful discussions. KH gratefully acknowledges support from the Academy of Finland (Project No. 115032). This work was funded in the UK by the STFC.

References

[1] H. Georgi and M. Machacek, *Doubly charged Higgs bosons*, *Nucl. Phys.* **B 262** (1985) 463 [SPIRES].

[2] K. Huitu, J. Maalampi, A. Pietila and M. Raidal, *Doubly charged Higgs at LHC*, *Nucl. Phys.* **B 487** (1997) 27 [hep-ph/9606311] [SPIRES];
K. Huitu, P.N. Pandita and K. Puolamaki, *Constraining the vacuum expectation values in naturally R-parity conserving supersymmetric models*, *Phys. Lett.* **B 415** (1997) 156 [hep-ph/9702415] [SPIRES]; *Mass of the lightest Higgs boson in supersymmetric left-right models*, *Phys. Lett.* **B 423** (1998) 97 [hep-ph/9708486] [SPIRES];
S. Chakrabarti, D. Choudhury, R.M. Godbole and B. Mukhopadhyaya, *Observing doubly charged Higgs bosons in photon photon collisions*, *Phys. Lett.* **B 434** (1998) 347 [hep-ph/9804297] [SPIRES];
K. Huitu, P.N. Pandita and K. Puolamaki, *Phenomenology of light Higgs bosons in supersymmetric left-right models*, hep-ph/9904388 [SPIRES];
K. Huitu, J. Laitinen, J. Maalampi and N. Romanenko, *Singly charged Higgses at linear collider*, *Nucl. Phys.* **B 598** (2001) 13 [hep-ph/0006261] [SPIRES];
S. Godfrey, P. Kalyniak and N. Romanenko, *Signatures of doubly charged Higgs bosons in $e\gamma$ collisions*, *Phys. Rev.* **D 65** (2002) 033009 [hep-ph/0108258] [SPIRES];
J. Maalampi and N. Romanenko, *Single production of doubly charged Higgs bosons at hadron colliders*, *Phys. Lett.* **B 532** (2002) 202 [hep-ph/0201196] [SPIRES];
S. Godfrey, P. Kalyniak and N. Romanenko, *Discovery potential for doubly charged Higgs bosons in e^+e^- collisions at LEP*, *Phys. Lett.* **B 545** (2002) 361 [hep-ph/0207240] [SPIRES];
A.G. Akeroyd and M. Aoki, *Single and pair production of doubly charged Higgs bosons at hadron colliders*, *Phys. Rev.* **D 72** (2005) 035011 [hep-ph/0506176] [SPIRES];
B. Mukhopadhyaya and S.K. Rai, *Associated single photons as signals for a doubly charged scalar at linear e^-e^- colliders*, *Phys. Lett.* **B 633** (2006) 519 [hep-ph/0508290] [SPIRES];
J.E. Cieza Montalvo, N.V. Cortez, J. Sa Borges and M.D. Tonasse, *Searching for doubly charged Higgs bosons at the LHC in a* 3-3-1 *model*, *Nucl. Phys.* **B 756** (2006) 1 [*Erratum ibid.* **B 796** (2008) 422] [hep-ph/0606243] [SPIRES];
T. Rommerskirchen and T. Hebbeker, *Study of pair-produced doubly charged Higgs bosons with a four-muonfinal state with the CMS detector*, *J. Phys.* **G 33** (2007) N47 [SPIRES];

JHEP05(2009)011

T. Han, B. Mukhopadhyaya, Z. Si and K. Wang, *Pair production of doubly-charged scalars: neutrino mass constraints and signals at the LHC*, *Phys. Rev.* **D 76** (2007) 075013 [arXiv:0706.0441] [SPIRES];
J.F. Gunion, C. Loomis and K.T. Pitts, *Searching for doubly charged Higgs bosons at future colliders*, hep-ph/9610237 [SPIRES];
I. Dorsner and I. Mocioiu, *Predictions from type-II see-saw mechanism in* SU(5), *Nucl. Phys.* **B 796** (2008) 123 [arXiv:0708.3332] [SPIRES];
F. del Aguila and J.A. Aguilar-Saavedra, *Distinguishing seesaw models at LHC with multi-lepton signals*, *Nucl. Phys.* **B 813** (2009) 22 [arXiv:0808.2468] [SPIRES].

[3] A.A. Johansen, N.G. Uraltsev and V.A. Khoze, *Heavy charged H bosons in the case of nonstandard Higgs sector*, *Sov. J. Nucl. Phys.* **46** (1987) 890 [*Yad. Fiz.* **46** (1987) 1502] [SPIRES].

[4] A. Kundu and B. Mukhopadhyaya, *A general Higgs sector: constraints and phenomenology*, *Int. J. Mod. Phys.* **A 11** (1996) 5221 [hep-ph/9507305] [SPIRES];
G.L. Kane, S.F. King and L.-T. Wang, *What will we learn if a Higgs boson is found?*, *Phys. Rev.* **D 64** (2001) 095013 [hep-ph/0010312] [SPIRES];
C.P. Burgess, J. Matias and M. Pospelov, *A Higgs or not a Higgs? What to do if you discover a new scalar particle*, *Int. J. Mod. Phys.* **A 17** (2002) 1841 [hep-ph/9912459] [SPIRES];
D. Choudhury, A. Datta and K. Huitu, *Z Z H coupling: a probe to the origin of EWSB?*, *Nucl. Phys.* **B 673** (2003) 385 [hep-ph/0302141] [SPIRES].

[5] For a recent review see J.F. Gunion and C. Hays, *Higgs triplets*, in *Workshop on CP studies and non-standard Higgs physics*, E. Accomando et al., hep-ph/0608079 [SPIRES], pg. 497.

[6] N. Arkani-Hamed, A.G. Cohen, E. Katz and A.E. Nelson, *The littlest Higgs*, *JHEP* **07** (2002) 034 [hep-ph/0206021] [SPIRES].

[7] V.A. Khoze, A.D. Martin and M.G. Ryskin, *Prospects for new physics observations in diffractive processes at the LHC and Tevatron*, *Eur. Phys. J.* **C 23** (2002) 311 [hep-ph/0111078] [SPIRES].

[8] FP420 R AND D collaboration, M.G. Albrow et al., *The FP420 R&D project: Higgs and new physics with forward protons at the LHC*, arXiv:0806.0302 [SPIRES].

[9] J.J. van der Bij, *Two loop large Higgs mass correction to vector boson masses*, *Nucl. Phys.* **B 248** (1984) 141 [SPIRES].

[10] J.J. van der Bij, *Does low-energy physics depend on the potential of a heavy Higgs particle?*, *Nucl. Phys.* **B 267** (1986) 557 [SPIRES].

[11] M.B. Einhorn and J. Wudka, *Screening of heavy Higgs radiative effects*, *Phys. Rev.* **D 39** (1989) 2758 [SPIRES].

[12] R. Barbieri, P. Ciafaloni and A. Strumia, *Two loop large Higgs mass corrections in all electroweak precision tests*, *Phys. Lett.* **B 317** (1993) 381 [SPIRES].

[13] V. Borodulin and G. Jikia, *Analytic evaluation of two-loop renormalization constants of enhanced electroweak strength in the Higgs sector of the standard model*, *Phys. Lett.* **B 391** (1997) 434 [hep-ph/9609447] [SPIRES].

[14] R. Akhoury, J.J. van der Bij and H. Wang, *Interplay between perturbative and non-perturbative effects in the stealthy Higgs model*, *Eur. Phys. J.* **C 20** (2001) 497 [hep-ph/0010187] [SPIRES].

JHEP05(2009)011

[15] R. Boughezal, J.B. Tausk and J.J. van der Bij, *Three-loop electroweak correction to the ρ parameter in the large Higgs mass limit*, *Nucl. Phys.* **B 713** (2005) 278 [hep-ph/0410216] [SPIRES].

[16] A.C. Longhitano, *Heavy Higgs bosons in the Weinberg-Salam model*, *Phys. Rev.* **D 22** (1980) 1166 [SPIRES].

[17] J. van der Bij and M.J.G. Veltman, *Two loop large Higgs mass correction to the ρ parameter*, *Nucl. Phys.* **B 231** (1984) 205 [SPIRES].

[18] J.F. Gunion, H.E. Haber, G.L. Kane and S. Dawson, *The Higgs hunter's guide*, BNL-41644 Westview Press, Boulder U.S.A. [SPIRES]; *Errata for the Higgs hunter's guide*, hep-ph/9302272 [SPIRES].

[19] J. Erler and P. Langacker, *Electroweak model and constraints on new physics*, in Particle Data Group collaboration, W.M. Yao et al., *Review of particle physics*, *J. Phys.* **G 33** (2006) 1 [SPIRES].

[20] M.-C. Chen, S. Dawson and C.B. Jackson, *Higgs triplets, decoupling and precision measurements*, *Phys. Rev.* **D 78** (2008) 093001 [arXiv:0809.4185] [SPIRES].

[21] M.S. Chanowitz and M. Golden, *Higgs boson triplets with $M_W = M_Z \cos\theta_\omega$*, *Phys. Lett.* **B 165** (1985) 105 [SPIRES].

[22] J.F. Gunion, R. Vega and J. Wudka, *Higgs triplets in the standard model*, *Phys. Rev.* **D 42** (1990) 1673 [SPIRES].

[23] J.F. Gunion, R. Vega and J. Wudka, *Naturalness problems for $\rho = 1$ and other large one loop effects for a standard model Higgs sector containing triplet fields*, *Phys. Rev.* **D 43** (1991) 2322 [SPIRES].

[24] J.R. Ellis, M.K. Gaillard and D.V. Nanopoulos, *A phenomenological profile of the Higgs boson*, *Nucl. Phys.* **B 106** (1976) 292 [SPIRES];
B.L. Ioffe and V.A. Khoze, *What can be expected from experiments on colliding e^+e^- beams with E approximately equal to* 100 *Gev?*, Leningrad-76-274 (1976) [*Sov. J. Part. Nucl.* **9** (1978) 50] [*Fiz. Elem. Chast. Atom. Yadra* **9** (1978) 118] [SPIRES].

[25] M. Aoki and S. Kanemura, *Unitarity bounds in the Higgs model including triplet fields with custodial symmetry*, *Phys. Rev.* **D 77** (2008) 095009 [arXiv:0712.4053] [SPIRES].

[26] H.E. Haber and H.E. Logan, *Radiative corrections to the $Zb\bar{b}$ vertex and constraints on extended Higgs sectors*, *Phys. Rev.* **D 62** (2000) 015011 [hep-ph/9909335] [SPIRES];
K. Cheung and D.K. Ghosh, *Triplet Higgs boson at hadron colliders*, *JHEP* **11** (2002) 048 [hep-ph/0208254] [SPIRES].

[27] D0 collaboration, W.-C. Yang, *Search for MSSM Higgs boson production in Di-τ final states with $L = 2.2$ fb^{-1} at the D0 detector*, arXiv:0810.3219 [SPIRES];
D0 collaboration, V.M. Abazov et al., *Search for Higgs bosons decaying to τ pairs in $p\bar{p}$ collisions with the D0 detector*, *Phys. Rev. Lett.* **101** (2008) 071804 [arXiv:0805.2491] [SPIRES].

[28] A. De Roeck, V.A. Khoze, A.D. Martin, R. Orava and M.G. Ryskin, *Ways to detect a light Higgs boson at the LHC*, *Eur. Phys. J.* **C 25** (2002) 391 [hep-ph/0207042] [SPIRES].

[29] J.R. Forshaw and M.H. Seymour, *Soft gluons and superleading logarithms in QCD*, arXiv:0901.3037 [SPIRES];
J.R. Forshaw and A. Pilkington, in *Hamburg* 2007, *Blois*07, *Forward physics and QCD*, pg. 130.

JHEP05(2009)011

[30] P.J. Bussey, *Detection of new states using forward proton tagging at the LHC*, arXiv:0809.1335 [SPIRES];
CMS collaboration, M. Grothe, *Forward detectors around the CMS interaction point at LHC and their physics potential*, *Nucl. Phys. Proc. Suppl.* **179-180** (2008) 173 [arXiv:0806.2977] [SPIRES].

[31] S. Heinemeyer et al., *Studying the MSSM Higgs sector by forward proton tagging at the LHC*, *Eur. Phys. J.* **C 53** (2008) 231 [arXiv:0708.3052] [SPIRES].

[32] S. Heinemeyer, V.A. Khoze, M.G. Ryskin, M. Tasevsky and G. Weiglein, *Central exclusive production of BSM Higgs bosons at the LHC*, arXiv:0811.4571 [SPIRES].

[33] B.E. Cox, F.K. Loebinger and A.D. Pilkington, *Detecting Higgs bosons in the bb decay channel using forward proton tagging at the LHC*, *JHEP* **10** (2007) 090 [arXiv:0709.3035] [SPIRES].

[34] V.A. Khoze, A.D. Martin and M. Ryskin, *Double diffractive processes in high resolution missing mass experiments at the Tevatron*, *Eur. Phys. J.* **C 19** (2001) 477 [*Erratum ibid.* **C 20** (2001) 599] [hep-ph/0011393] [SPIRES].

[35] A. Kaidalov, V.A. Khoze, A.D. Martin and M. Ryskin, *Extending the study of the Higgs sector at the LHC by proton tagging*, *Eur. Phys. J.* **C 33** (2004) 261 [hep-ph/0311023] [SPIRES].

[36] J.R. Ellis, J.S. Lee and A. Pilaftsis, *Diffraction as a CP and lineshape analyzer for MSSM Higgs bosons at the LHC*, *Phys. Rev.* **D 71** (2005) 075007 [hep-ph/0502251] [SPIRES].

[37] J.R. Forshaw, J.F. Gunion, L. Hodgkinson, A. Papaefstathiou and A.D. Pilkington, *Reinstating the 'no-lose' theorem for NMSSM Higgs discovery at the LHC*, *JHEP* **04** (2008) 090 [arXiv:0712.3510] [SPIRES].

[38] V.A. Khoze, A.D. Martin and M.G. Ryskin, *Can the Higgs be seen in rapidity gap events at the Tevatron or the LHC?*, *Eur. Phys. J.* **C 14** (2000) 525 [hep-ph/0002072] [SPIRES].

[39] V.A. Khoze, A.D. Martin and M.G. Ryskin, *Soft diffraction and the elastic slope at Tevatron and LHC energies: a multipomeron approach*, *Eur. Phys. J.* **C 18** (2000) 167 [hep-ph/0007359] [SPIRES].

[40] M.G. Ryskin, A.D. Martin and V.A. Khoze, *Soft diffraction at the LHC: a partonic interpretation*, *Eur. Phys. J.* **C 54** (2008) 199 [arXiv:0710.2494] [SPIRES];
E.G.S. Luna, V.A. Khoze, A.D. Martin and M.G. Ryskin, *Diffractive dissociation re-visited for predictions at the LHC*, *Eur. Phys. J.* **C 59** (2009) 1 [arXiv:0807.4115] [SPIRES].

[41] M.G. Ryskin, A.D. Martin and V.A. Khoze, *Soft processes at the LHC, I: multi-component model*, *Eur. Phys. J.* **C 60** (2009) 249 [arXiv:0812.2407] [SPIRES]; *Soft processes at the LHC, II: soft-hard factorization breaking and gap survival*, *Eur. Phys. J.* **C 60** (2009) 265 [arXiv:0812.2413] [SPIRES].

[42] V.A. Khoze, A.D. Martin and M.G. Ryskin, *Early LHC measurements to check predictions for central exclusive production*, *Eur. Phys. J.* **C 55** (2008) 363 [arXiv:0802.0177] [SPIRES].

[43] V.A. Khoze, A.D. Martin, M.G. Ryskin and W.J. Stirling, *Double-diffractive χ meson production at the hadron colliders*, *Eur. Phys. J.* **C 35** (2004) 211 [hep-ph/0403218] [SPIRES].

JHEP05(2009)011

[44] A.D. Martin, V.A. Khoze and M.G. Ryskin, *Rapidity gap survival probability and total cross sections*, arXiv:0810.3560 [SPIRES]; *Diffractive processes at the LHC*, *AIP Conf. Proc.* **1105** (2009) 252 [arXiv:0811.1481] [SPIRES].

[45] V.A. Khoze, A.D. Martin and M.G. Ryskin, *On the role of hard rescattering in exclusive diffractive Higgs production*, *JHEP* **05** (2006) 036 [hep-ph/0602247] [SPIRES].

[46] CDF collaboration, T. Aaltonen et al., *Observation of exclusive Dijet production at the Fermilab tevatron $p^-\bar{p}$ collider*, *Phys. Rev.* **D 77** (2008) 052004 [arXiv:0712.0604] [SPIRES].

[47] CDF collaboration, T. Aaltonen et al., *Search for exclusive $\gamma\gamma$ production in hadron-hadron collisions*, *Phys. Rev. Lett.* **99** (2007) 242002 [arXiv:0707.2374] [SPIRES].

[48] CDF collaboration, M.G. Albrow, *Central exclusive production at the Tevatron*, arXiv:0812.0612 [SPIRES].

[49] A.B. Kaidalov, V.A. Khoze, A.D. Martin and M.G. Ryskin, *Probabilities of rapidity gaps in high-energy interactions*, *Eur. Phys. J.* **C 21** (2001) 521 [hep-ph/0105145] [SPIRES].

[50] J. Bartels, S. Bondarenko, K. Kutak and L. Motyka, *Exclusive Higgs boson production at the LHC: hard rescattering corrections*, *Phys. Rev.* **D 73** (2006) 093004 [hep-ph/0601128] [SPIRES].

[51] USCMS collaboration, M. Albrow et al., *Forward physics with rapidity gaps at the LHC*, arXiv:0811.0120 [SPIRES].

[52] P.J. Bussey and W. Plano, *FPTrack*, to be published.

[53] J. Monk and A. Pilkington, *ExHuME: a Monte Carlo event generator for exclusive diffraction*, *Comput. Phys. Commun.* **175** (2006) 232 [hep-ph/0502077] [SPIRES].

[54] J. Pumplin et al., *New generation of parton distributions with uncertainties from global QCD analysis*, *JHEP* **07** (2002) 012 [hep-ph/0201195] [SPIRES].

[55] A.G. Shuvaev, V.A. Khoze, A.D. Martin and M.G. Ryskin, *One-loop $gg \to b\bar{b}$ effects in the main irreducible background to exclusive $H \to b\bar{b}$ production at the LHC*, *Eur. Phys. J.* **C 56** (2008) 467 [arXiv:0806.1447] [SPIRES].

[56] ATLAS collaboration, *b-tagging performance*, in *ATLAS: Detector and physics performance technical design report*, volume 1, CERN-LHCC-99-14, (1999), pg. 317 [SPIRES].

[57] V.A. Khoze, M.G. Ryskin and W.J. Stirling, *On radiative QCD backgrounds to exclusive $H \to b\bar{b}$ production at the LHC and a photon collider*, *Eur. Phys. J.* **C 48** (2006) 477 [hep-ph/0607134] [SPIRES].

[58] V.A. Khoze, A.D. Martin and M.G. Ryskin, *Insight into double-Pomeron-exchange Higgs production and backgrounds*, *Phys. Lett.* **B 650** (2007) 41 [hep-ph/0702213] [SPIRES].

[59] G. Corcella et al., *HERWIG* 6.5 *release note*, hep-ph/0210213 [SPIRES].

[60] J.M. Butterworth, J.R. Forshaw and M.H. Seymour, *Multiparton interactions in photoproduction at HERA*, *Z. Phys.* **C 72** (1996) 637 [hep-ph/9601371] [SPIRES].

[61] C.M. Buttar et al., *The underlying event*, in S. Alekhin et al., *HERA and the LHC — a workshop on the implications of HERA for LHC physics: proceedings part B*, hep-ph/0601013 [SPIRES].

JHEP05(2009)011

[62] ATLAS collaboration, *Electromagnetic calorimetry*, in *ATLAS: Detector and physics performance technical design report*, volume 1, CERN-LHCC-99-14, (1999), pg. 99 [SPIRES].

[63] P.J. Bussey, T.D. Coughlin, J.R. Forshaw and A.D. Pilkington, *Central exclusive production of longlived gluinos at the LHC*, *JHEP* **11** (2006) 027 [hep-ph/0607264] [SPIRES].

[64] V.A. Khoze, A.D. Martin and M.G. Ryskin, *Central jet production as a probe of the perturbative formalism for exclusive diffraction*, *Eur. Phys. J.* **C 48** (2006) 467 [hep-ph/0605113] [SPIRES].

[65] M. Grothe et al., *Triggering on forward physics*, CERN-CMS-NOTE-2006-054 [SPIRES].

[66] CMS & TOTEM DIFFRACTIVE AND FORWARD PHYSICS WORKING GROUP collaboration, M. Albrow et al., *Prospects for diffractive and forward physics at the LHC*, CERN-LHCC 2006-039 [CERN-LHCC-G-124] [CERN-CMS-NOTE-2007-002] (2006).

[67] S.N. White, *On the correlation of subevents in the ATLAS and CMS/Totem experiments*, arXiv:0707.1500 [SPIRES].

[68] T. Han, B. Mukhopadhyaya, Z. Si and K. Wang, *Pair production of doubly-charged scalars: neutrino mass constraints and signals at the LHC*, *Phys. Rev.* **D 76** (2007) 075013 [arXiv:0706.0441] [SPIRES].

[69] N. Schul and K. Piotrzkowski, *Detection of two-photon exclusive production of supersymmetric pairs at the LHC*, *Nucl. Phys. Proc. Suppl.* **179-180** (2008) 289 [arXiv:0806.1097] [SPIRES].

JHEP05(2009)011